Current Biology 18, 1943–1948, December 23, 2008 ©2008 Elsevier Ltd All rights reserved DOI 10.1016/j.cub.2008.10.065

Report

Arabidopsis Phyllotaxis Is Controlled by the Methyl-Esterification Status of Cell-Wall Pectins

Alexis Peaucelle,[1,*] Romain Louvet,[2] Jorunn N. Johansen,[1] Herman Höfte,[1] Patrick Laufs,[1] Jérome Pelloux,[2] and Grégory Mouille[1,*]

[1]Laboratoire de Biologie Cellulaire
Institut Jean-Pierre Bourgin
INRA Centre de Versailles-Grignon
Route de St Cyr
78026 Versailles
France

[2]EA3900-BioPI Biologie des plantes et Contrôle des Insectes Ravageurs
Université de Picardie
33 Rue St Leu
80039 Amiens
France

Summary

Plant organs are produced from meristems in a characteristic pattern. This pattern, referred to as phyllotaxis, is thought to be generated by local gradients of an information molecule, auxin [1–6]. Some studies propose a key role for the mechanical properties of the cell walls in the control of organ outgrowth [7–12]. A major cell-wall component is the linear α-1-4-linked D-GalAp pectic polysaccharide homogalacturonan (HG), which plays a key role in cell-to-cell cohesion [13, 14]. HG is deposited in the cell wall in a highly (70%–80%) methyl-esterified form and is subsequently de-methyl-esterified by pectin methyl-esterases (PME, EC 3.1.1.11). PME activity is itself regulated by endogenous PME inhibitor (PMEI) proteins [15]. PME action modulates cell-wall-matrix properties and plays a role in the control of cell growth [16–18]. Here, we show that the formation of flower primordia in the *Arabidopsis* shoot apical meristem is accompanied by the de-methyl-esterification of pectic polysaccharides in the cell walls. In addition, experimental perturbation of the methyl-esterification status of pectins within the meristem dramatically alters the phyllotactic pattern. These results demonstrate that regulated de-methyl-esterification of pectins is a key event in the outgrowth of primordia and possibly also in phyllotactic patterning.

Results

To analyze the methyl-esterification status of HG at successive stages of primordia formation in *Arabidopsis* inflorescence meristems, we first used the monoclonal antibody 2F4, which specifically labels de-methyl-esterified and not methyl-esterified HG [19]. Successive transverse sections through inflorescence meristems were labeled with 2F4 (Figure 1). As described previously for *Sinapis alba* apical meristems [19], the center of the meristem dome of wild-type plants remained unlabeled (Figure 1A), whereas chemically de-esterified control slides showed strong labeling (Figure S1 available online). This indicates that in this zone, cell walls contained pectins that were primarily methyl-esterified. In contrast, 2F4 labeling was observed in the walls of young (stage p1 to p3) and incipient primordia (I1 and very weakly in I2) (Figure 1A), suggesting that HG was selectively de-methyl-esterified during primordia formation before their outgrowth. This cell-wall modification is among the first events in primordia differentiation. We next analyzed the functional significance of the reduced pectin methyl-esterification status for primordia formation. The enzyme responsible for the de-methyl-esterification of HG in vivo is PME. A large gene family encoding PMEs exists in *Arabidopsis* (66 members) [20], some members of which are expressed in the apical-meristem dome (data not shown). So far, knockout mutants in three meristem-expressed PMEs (*At3g05620*, *At3g27980*, and *At5g47500*) did not show a visible phenotype (data not shown). This may be the result of functional redundancy within the PME family. We therefore adopted an alternative method based on the use of a PMEI to inhibit PME activity. *Arabidopsis* encodes 69 putative PMEIs (J.P., unpublished data), at least one of which (*At5g20740*, henceforward referred to as *PMEI3*) is expressed in the apical meristem (data not shown). We analyzed ten independent *Arabidopsis* lines transgenic for an alcohol-inducible *PMEI3* construct. Upon alcohol induction, two lines (PMEI.H1 and H2) showed high *PMEI3* expression (respectively 9- and 3.5-fold higher than wild-type) and one line (PMEI.M) showed intermediate expression (1.3-fold higher than wild-type), whereas seven lines showed no *PMEI3* upregulation (Figure S2). To verify the in vivo activity of PMEI3, we used 2F4 to label sections through meristems of PMEI.H1. Eighteen hours after ethanol induction, 2F4 labeling was significantly reduced throughout the meristem dome (in all of ten T2 plants investigated, Figure 1B), compared to control plants (Figure 1A), whereas the labeling of older primordia remained unaffected. This shows that overexpression of *PMEI3* leads to hyper-methyl-esterification of HG and strongly suggests that PMEI3, as expected, inhibits PME activity in vivo. Next, we investigated the meristem phenotype of the ten independent transformants grown for 6 days in the continuous presence of alcohol. In PMEI.H1 and H2, the formation of lateral organs was suppressed in the inflorescence meristem as shown by the naked PIN-like meristem (Figure 2B) [21]. In addition, the floral meristem that had been initiated just before the ethanol induction produced abnormal flowers lacking lateral organs (sepals, petals, and stamens) indicating that the formation of both floral and flower-organ primordia was inhibited (Figure 2E). In PMEI.M, newly formed primordia were cylindrical (Figure 2D) and did not develop further into flowers. Cylindrical primordia were also observed in PMEI.H1 and H2 in the presence of suboptimal concentrations of alcohol (data not shown). The meristem phenotype was fully reversible in all transformants as shown by the reappearance of lateral organs after removal of the alcohol (Figure S3), indicating that the meristem remained fully functional. Intriguingly, during the reversion, newly formed primordia showed abnormal phyllotaxis and were frequently dramatically enlarged (Figure 2E). As expected, the remaining seven lines in which PMEI3 was not induced did not show

*Correspondence: alexis.peaucelle@versailles.inra.fr (A.P.), gregory.mouille@versailles.inra.fr (G.M.)

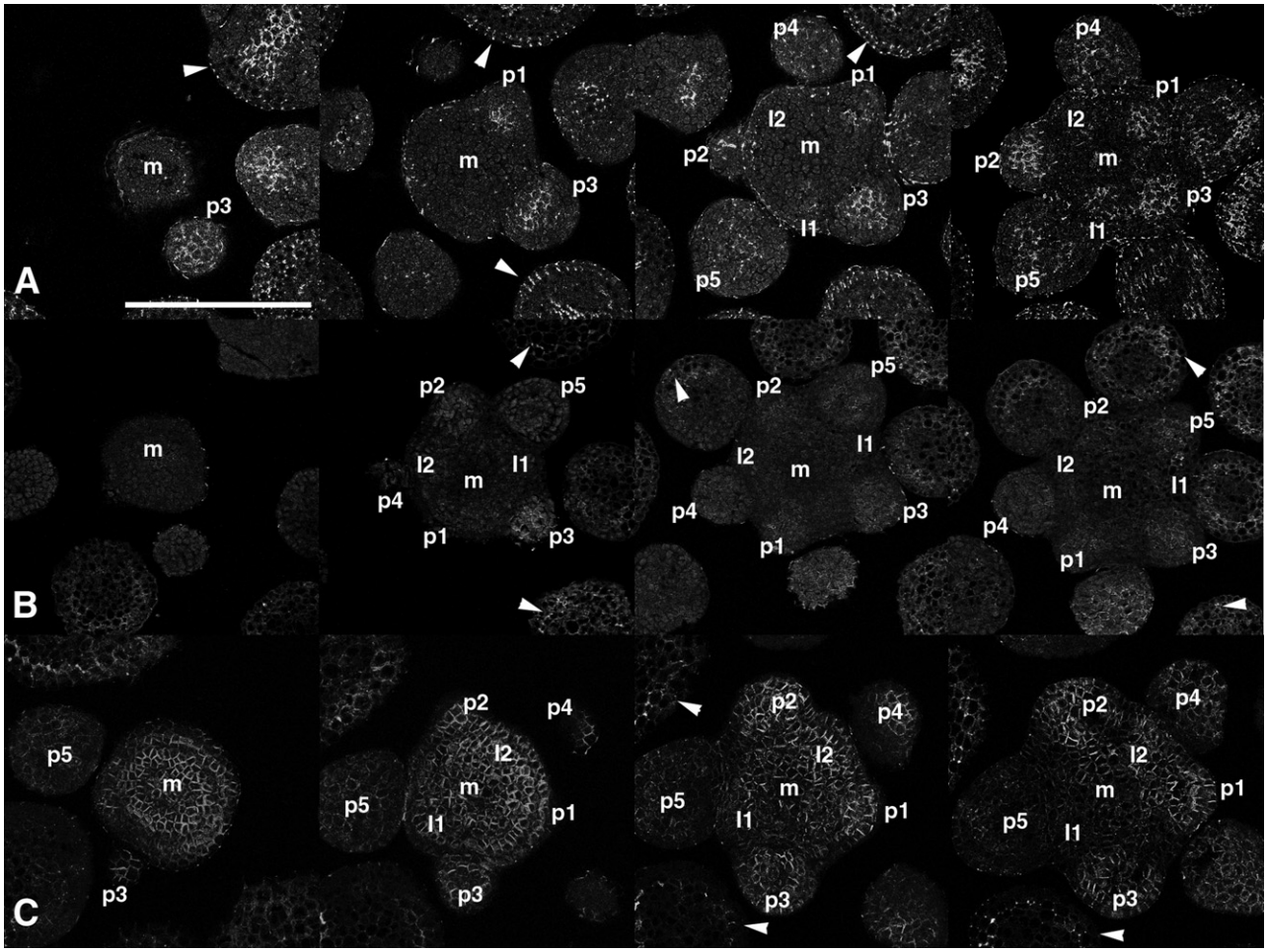

Figure 1. Pectins Are De-methyl-esterified during Primordia Formation

Immunolabeling of de-methyl-esterified homogalacturonan with monoclonal antibody 2F4 on four successive cross sections from the top to the base (from left to right) of a single representative wild-type (A), transgenic *Arabidopsis* lines transformed with an alcohol-inducible *PMEI3* construct (B), or *PME5* construct (C) inflorescence meristem. Each image has been acquired with confocal laser microscopy and corresponds to one optical section in the middle of a 7-μm-thick cross section. As shown in (A), in the wild-type inflorescence 2F4 labels cell walls (white staining) within growing primordia (p1, p2, and p3) and at the position of the incipient primordia (I1) and very weakly in the incipient primordia I2 but not in the central zone of the meristem (m). In differentiated tissues, de-methyl-esterified pectin epitopes are also visible (indicated by arrowheads). Similar results were obtained with 14 other meristems in four independent labeling experiments (data not shown). As shown in (B), in transgenic *Arabidopsis PMEI.H1* lines transformed with the *35S::ALCR ALCA::PMEI3* construct; 18 hr after induction, a strong reduction of the 2F4 labeling could be observed in the old primordias (p2, p3, p4, and p5). No epitopes could be found in the young primordia (p1) and the incipient primordia (I1 and I2). In differentiated tissues, de-methyl-esterified pectin epitopes are visible, as in the wild-type (indicated by arrowheads). Similar results were obtained with 13 other meristems in four independent experiments (data not shown). As shown in (C), 18 hr after induction, the plants transformed with the *35S::ALCR ALCA::PME5* construct present a strong increase in the 2F4 epitopes present. De-methyl-esterified pectin epitopes are present not only in primordia and incipient primordia (p1, p2, p3, I1, and I2) but also in the meristem (m). In differentiated tissues, de-methyl-esterified pectin epitopes are also visible (indicated by arrowheads). Similar results were obtained with 12 other meristems in three independent labeling experiments (data not shown). The scale bar represents 100 μm.

a phenotype (data not shown). The stem length measured 4 weeks after induction on F2 plants was comparable in induced and noninduced plants (respectively 19.5 ± 3.5 cm and 20 ± 3.6 cm), indicating that only lateral organ formation and not stem elongation was affected by PMEI overexpression. Together, these experiments show that de-methyl-esterification of HG not only accompanies but is also required for primordia formation in the inflorescence meristem.

We next investigated whether enhanced de-methyl-esterification of HG could lead to ectopic primordia formation. For this purpose, we first positioned individual sepharose beads loaded with citrus PME onto the inflorescence meristem (Figure 3A). Interestingly, 18 hr later, ectopic bulges had formed at the position of the beads (Figure 3B) in nine of the ten meristems analyzed (one meristem was wounded during bead application) and not in the control experiment (ten meristems treated with denatured PME). The ectopic bulges further developed into normal floral meristems and formed fully grown flowers (Figure 3C). As shown in Figures 3A–3G, bulges did not necessarily form at the position of the future primordia, suggesting that pectin de-methyl-esterification can trigger de novo formation of primordia rather than merely accelerating the outgrowth of primordia along a pre-existing pattern. Because the application of individual beads onto a defined spot on the very small *Arabidopsis* apical meristem turned out to be very delicate and laborious, the experiment was simplified so that more quantitative data could be obtained. Several beads were applied on top of the meristem of a line carrying

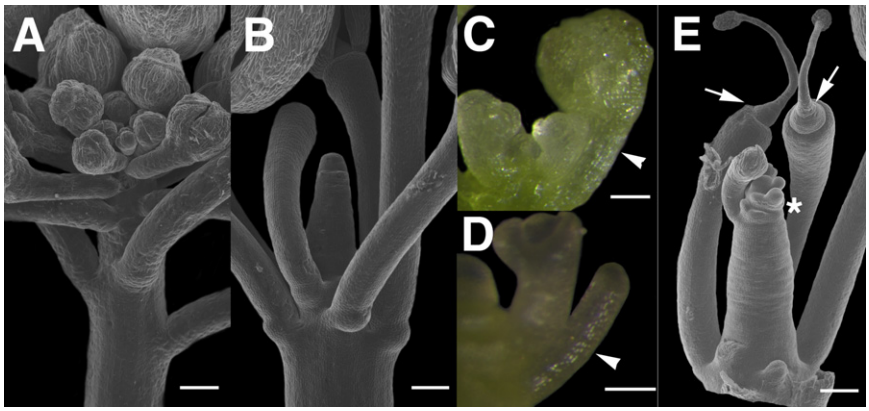

Figure 2. Inhibition of Pectin De-methyl-esterification in the Meristem Prevents Primordia Formation

Phenotype upon transient ethanol-induced overexpression of putative PME inhibitor *PMEI3* in the line PMEI.H1 (B, D, and E) compared to the wild-type (A and C). Organ formation is suppressed after 6 days in the presence of ethanol and a PIN-like meristem is visible (B). Primordia initiated just before the ethanol induction develop into abnormal flowers with a carpeloïd structure at the center but lacking lateral organs (sepals, petals, and stamens) ([E], indicated by arrowheads). Low-level induction of *PMEI3* in line PMEI.M causes the formation of cylindrical primordia ([D], indicated by an arrowhead) thinner than wild-type primordia at the same developmental stage ([C], indicated by an arrowhead). One day after ethanol removal in PMEI.H1, dramatically enlarged primordia have appeared at ectopic positions ([E], marked by an asterisk). Scale bars represent 100 μm.

a *pLFY::GUS* primordia marker (Figures 3D–3G). Two days later, we measured the angle between the successive, GUS-stained primordia. Abnormal phyllotaxis (at least one divergent angle higher than 182° or lower than 92°) was observed in 17 out of 19 apices treated with active PME (Figures 3D and 3E) and only in one out of ten control meristems treated with heat-denaturated PME (Figures 3F and 3G). In addition, in PME-treated plants, 44% of the primordia were formed in an abnormal position (Figure 3E) compared to less than 2% in the control experiment (Figure 3G). Several primordia at the same developmental stage were frequently observed in PME-treated plants, indicating that the plastochrone (timing of primordia formation) was affected (Figure 3D). All the primordia developed normally and formed fertile flowers, indicating that the whole lateral organ developmental program was activated by the PME application. To rule out that the abnormal phyllotaxis was the result of a change in meristem size, we compared the meristem diameter of PME-treated and control plants, which did not differ significantly (respectively 59 ± 6.9 μm and 58 ± 7.5 μm). Together, these results show that application of PME onto the meristem is sufficient to induce the formation of ectopic primordia, without altering the global meristem organization. Interestingly, although PME-loaded beads were deposited onto the whole meristem, formation of the ectopic primordia remained restricted to the periphery of the meristem, suggesting that additional factors prevent primordia formation in the central dome. To confirm the role of pectin de-methyl-esterification in primordia formation, we studied the phyllotaxis upon ectopic expression of an *Arabidopsis* gene (*At5g47500*) encoding a putative PME (hereafter referred to as PME5), which in the wild-type is expressed in meristem primordia (data not shown). We first used the alcohol-inducible system combined with the *35S* promoter. After ethanol induction, the *35S::ALCR ALCA::PME5* line showed increased 2F4 labeling in the meristem (Figure 1C) and a strongly perturbed phyllotactic pattern (Figures 3H and 3I). In fact, 49% of the primordia were formed in an abnormal position (Figure 3I) compared to less than 2% in the control experiment (Figure 3G). This confirms that PME activity is sufficient to induce the initiation of ectopic primordia. This was further confirmed by use of a construct expressing PME5 from an alcohol-inducible version of the *UFO* promoter (*UFO::ALCR ALCA::PME5*). This construct specifically expresses PME5 in the peripheral region of the meristem after ethanol induction (data not shown). Again, important modifications of the phyllotactic pattern were observed in inflorescences of six out of seven independent transgenic lines after 3 weeks of growth in the presence of ethanol (Figures 3J and 3K). No such changes were observed in ethanol-induced control lines.

Together, the results of this study show that pectin de-methyl-esterification occurs during primordia formation and is necessary and sufficient to trigger the initiation of organs in inflorescence meristems.

Discussion

Two alternative models have been proposed to explain the regular pattern of morphogenesis at the shoot apex, and each model emphasize either the involvement of mechanical forces or gradients of an information molecule, auxin. Current models predict the position of organ primordia based on auxin gradients, which in turn are generated by the auxin-dependent polarized localization of auxin efflux carriers within the meristem epidermis [1–6]. At the same time, other studies have shown that experimental manipulation of the mechanical properties of the walls of subsets of meristematic cells, through local expression of the cell-wall-lubricating protein expansin, can promote the formation of normal organs at abnormal positions in the meristem. This indicates that the entire sequence of events leading to leaf formation can be triggered by a local increase in cell-wall extensibility [7, 8]. Closer inspection, however, shows that the latter results are not necessarily in contradiction with the auxin-patterning models. Indeed, the ectopic organs always formed at the position of a future organ initium, which according to the models is determined by the position of the local auxin maximum. In other words, the changes in cell-wall mechanics affected the outgrowth of the organ primordium but not its positioning. In this study, we showed that selective pectin de-methyl-esterification is required and sufficient for primordia outgrowth at the meristem periphery. We thus confirm that cell-wall changes can trigger organ outgrowth, and we also show that these cell-wall changes actually occur during normal primordia formation. In addition, PME treatment, in contrast to ectopic expansin application, appeared to overrule the predetermined pattern of initia. This is suggested by the simultaneous appearance of more than one primordium on the same side of the meristem and the highly variable divergence angles observed upon PME

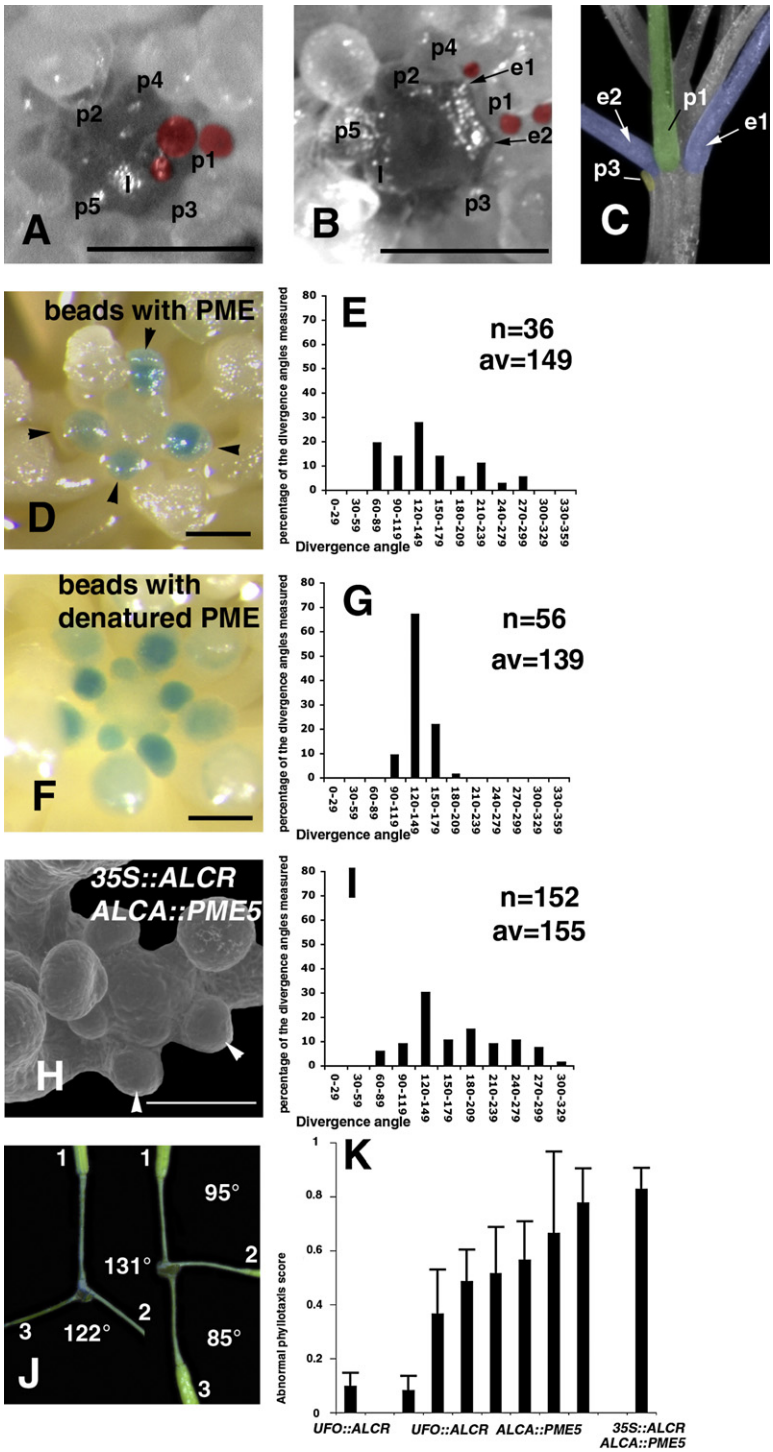

Figure 3. Ectopic Organs Induced by Pectin Methyl-Esterase

(A–C) Ectopic bulges form on the meristem 18 hr after positioning of beads (red false color) loaded with citrus PME. The same inflorescence meristem is shown immediately after application of the beads (A), 18 hr later (B), and 18 days later (C). Two ectopic bulges have formed next to the beads ([B], indicated by arrowheads e1 and e2), which further develop into normal flowers ([C], blue false color). In between the two flowers, the p1 primordium also has developed into a normal flower ([C], green false color). Primordium number p3 did not further develop as it was wounded during the observation 18 hr after application ([C], yellow false color). The position of the beads was slightly shifted during the removal of primordium p6, which used to cover p1.

(D–I) Ectopic PME activity alters phyllotaxis. Abnormal position and timing of primordia was observed 2 days after deposition on the meristem of beads loaded with active PME (D and E). This was not the case when using beads loaded with denatured PME (F and G). Primordia express the reporter gene GUS from the primordia-specific promoter LFY and are stained in blue (D and F). The 12 classes of 30° divergence angles between two successive primordia show a broad distribution in meristems treated with active PME (E) compared to the normal narrow distribution centered on 137.5° when denatured PME was used (G). The total number of angles measured (n), averages (av), and standard deviations are shown.

(H and I) Phyllotaxis is perturbed upon ethanol-induced expression of PME in the meristem. Similar results were obtained with ten meristems in two independent beads application experiments. (H) shows a SEM picture of a meristem containing *35S::ALCR ALCA::PME5* construct, 24 hr after ethanol induction. (I) shows distribution of the divergence angles.

(J and K) Phyllotaxis is perturbed upon alcohol induced expression of *Arabidopsis* PME5 (*At5g47500*) under the control of the meristem-specific UFO promoter. In (H), abnormal phyllotaxis was observed upon ectopic PME5 expression (right) and not in control plants (left). Scale bars represent 100 μm. In (I), phyllotaxis scores calculated for control plants and eight independent transformants are shown. Error bars correspond to standard deviation.

application or ectopic expression of a putative *PME* gene (*PME5*, Figure 3).

In summary, this study shows that the modification of cell-wall polymers not only is required and sufficient for primordia formation but also appears to influence the patterning process within the meristem. This raises new questions that may orient future research. First, what is the mechanism by which HG de-methyl-esterification causes primordia initiation? Pectin de-methyl-esterification has been implicated previously in the control of cell elongation in the pollen tube [22, 23] and the hypocotyl [24]. In both cases, increased de-methyl-esterification was correlated with reduced growth, which is the opposite of what was shown in this study. One possibility is that, depending on the context, de-methyl-esterification can induce opposing changes in the visco-elastic properties of the cell-wall composite. De-methyl-esterification of pectins uncovers carboxyl groups that can crosslink through calcium bridges and thus rigidify the cell wall. In the absence of calcium, however, de-methyl-esterification is expected to render pectins, and perhaps the cell-wall composite, more fluid. In this context, it will be interesting to quantify extracellular calcium in the meristem. De-methyl-esterification also renders HG susceptible to degradation by polygalacturonases, and such degradation in turn may increase the pore size of the cell wall and the accessibility of growth-promoting hydrolytic enzymes and expansins to wall polymers (discussed in [25]). Alternatively, the attack of de-methyl-esterified HG by endogenous polygalacturonases may generate oligo-galacturonides (OGA). Although certain OGA have biological activity [26], preliminary experiments failed to reveal an effect of OGA on primordia outgrowth [7]. Second, what is the relation between auxin patterning and

PME activity? In this context it will be interesting to investigate whether PME activity is regulated by auxin and to what extent PME-induced cell-wall changes affect auxin fluxes within the meristem.

Experimental Procedures

Plant Material and Growth Conditions

The R1 R2 recombination cassette (Gateway technology, Invitrogen) was introduced between the pAlcA ethanol inducible promoter and the 35S terminator of pL4 plasmid. The pAlcA-R1-R2-t35S cassette was recovered after a HindIII digestion and ligated into the binary vector pEC2 that contains a basta resistance cassette for plant-transformation selection. The *PME-5* and *PMEI-3* cDNAs were then introduced in this vector.

T1 transformed plants were obtained as described in Deveaux et al. [27] its progeny is referred as T2. The UFO::ALCR alcA::GUS and 35S::ALCR alcA::GFP 23 lines have been described previously. Plant growth in controlled chambers was conducted according to Laufs et al. [28] and ethanol induction according to Deveaux et al. [27].

Meristematic-Phyllotaxis Measurements

Meristematic-phyllotaxis measurements as well as digital pictures were acquired as described in Peaucelle et al. [29].

Immunolabeling of Unesterified Homogalacturonans

Sample preparation, sectioning, immunolabelling and imaging was performed as described by de Reuille et al. and Liners et al. [4, 30]. Since the 2F4 monoclonal antibodies only recognize Ca^{2+} cross-linked de-methylesterified pectins, all immuno-labelings were carried out using a buffer containing 0.5 M $CaCl_2$ in the presence of milk as described by Liners et al. [4, 30].

Pectin Methyl-Esterase Treatment

Beads (sephacrylHR S300 Pharmacia) were loaded with pectin methylesterase (PME) (Pectinesterase, from Orange peel P5400-1KU 065K7435 Sigma-Aldrich) by incubation overnight at 4°C in 1 M Phosphate buffer at pH 7 containing 1 U/100 μl PME. Denatured PME was obtained by heating at 100°C for 20 min and overnight heating at 70°C. A small number of beads (one to five) were picked up with forceps. This step drained the beads through capillarity on the forceps. One to twenty beads were positioned on nondissected apices. Meristems were covered with a 1.5 ml microfuge tube so that desiccation was prevented.

Supplemental Data

Supplemental Data include three figures and can be found with this article online at http://www.current-biology.com/supplemental/S0960-9822(08)01534-0.

Acknowledgments

Yves Couder and Steffen Bohn are thanked for fruitful discussions. Jan Traas and Elliot Meyerowitz are thanked for constructive remarks. Bruno Letarnec is thanked for taking care of the plants and Séverine Dominichi is thanked for helpful advice for scanning electron microscopy. Pierre Van Cutsem is thanked for providing the 2F4 antibodies. This work was funded in part by Human Frontiers Science Program grant n°RGP0062/2005-C and EC, FP6 grants n° 512265 (WALLNET) and n° 037704 (AGRON-OMICS) to H.H.

Received: August 19, 2008
Revised: October 3, 2008
Accepted: October 24, 2008
Published online: December 18, 2008

References

1. Vernoux, T., Kronenberger, J., Grandjean, O., Laufs, P., and Traas, J. (2000). PIN-FORMED 1 regulates cell fate at the periphery of the shoot apical meristem. Development *127*, 5157–5165.
2. Reinhardt, D., Mandel, T., and Kuhlemeier, C. (2000). Auxin regulates the initiation and radial position of plant lateral organs. Plant Cell *12*, 507–518.
3. Heisler, M.G., Ohno, C., Das, P., Sieber, P., Reddy, G.V., Long, J.A., and Meyerowitz, E.M. (2005). Patterns of auxin transport and gene expression during primordium development revealed by live imaging of the Arabidopsis inflorescence meristem. Curr. Biol. *15*, 1899–1911.
4. de Reuille, P.B., Bohn-Courseau, I., Ljung, K., Morin, H., Carraro, N., Godin, C., and Traas, J. (2006). Computer simulations reveal properties of the cell-cell signaling network at the shoot apex in Arabidopsis. Proc. Natl. Acad. Sci. USA *103*, 1627–1632.
5. Smith, R.S., Guyomarc'h, S., Mandel, T., Reinhardt, D., Kuhlemeier, C., and Prusinkiewicz, P. (2006). A plausible model of phyllotaxis. Proc. Natl. Acad. Sci. USA *103*, 1301–1306.
6. Jonsson, H., Heisler, M.G., Shapiro, B.E., Meyerowitz, E.M., and Mjolsness, E. (2006). An auxin-driven polarized transport model for phyllotaxis. Proc. Natl. Acad. Sci. USA *103*, 1633–1638.
7. Fleming, A., McQueen-Mason, S., Mandel, T., and Kuhlemeier, C. (1997). Induction of leaf primordia by the cell wall protein expansin. Science *276*, 1415–1418.
8. Pien, S., Wyrzykowska, J., McQueen-Mason, S., Smart, C., and Fleming, A. (2001). Local expression of expansin induces the entire process of leaf development and modifies leaf shape. Proc. Natl. Acad. Sci. USA *98*, 11812–11817.
9. Reinhardt, D., Wittwer, F., Mandel, T., and Kuhlemeier, C. (1998). Localized upregulation of a new expansin gene predicts the site of leaf formation in the tomato meristem. Plant Cell *10*, 1427–1437.
10. Couder, Y., Gerard, N., and Rabaud, M. (1986). Narrow fingers in the Saffman-Taylor instability. Phys. Rev. A *34*, 5175–5178.
11. Green, P.B., and Poethig, S. (1982). Biophysics of the extension and initiation of plant organs. In Developmental Order: Its Origin and Regulation, A.R. Liss, ed. (Hoboken, NJ: John Wiley and Sons), pp. 485–509.
12. Wyrzykowska, J., Pien, S., Shen, W.H., and Fleming, A.J. (2002). Manipulation of leaf shape by modulation of cell division. Development *129*, 957–964.
13. Bouton, S., Leboeuf, E., Mouille, G., Leydecker, M.T., Talbotec, J., Granier, F., Lahaye, M., Hofte, H., and Truong, H.N. (2002). QUASIMODO1 encodes a putative membrane-bound glycosyltransferase required for normal pectin synthesis and cell adhesion in Arabidopsis. Plant Cell *14*, 2577–2590.
14. Mouille, G., Ralet, M.C., Cavelier, C., Eland, C., Effroy, D., Hematy, K., McCartney, L., Truong, H.N., Gaudon, V., Thibault, J.F., et al. (2007). Homogalacturonan synthesis in Arabidopsis thaliana requires a Golgi-localized protein with a putative methyltransferase domain. Plant J. *50*, 605–614.
15. Juge, N. (2006). Plant protein inhibitors of cell wall degrading enzymes. Trends Plant Sci. *11*, 359–367.
16. Derbyshire, P., McCann, M.C., and Roberts, K. (2007). Restricted cell elongation in Arabidopsis hypocotyls is associated with a reduced average pectin esterification level. BMC Plant Biol. *7*, 31.
17. Lionetti, V., Raiola, A., Camardella, L., Giovane, A., Obel, N., Pauly, M., Favaron, F., Cervone, F., and Bellincampi, D. (2007). Overexpression of pectin methylesterase inhibitors in Arabidopsis restricts fungal infection by Botrytis cinerea. Plant Physiol. *143*, 1871–1880.
18. Pelloux, J., Rusterucci, C., and Mellerowicz, E.J. (2007). New insights into pectin methylesterase structure and function. Trends Plant Sci. *12*, 267–277.
19. Sobry, S., Havelange, A., and Van Cutsem, P. (2005). Immunocytochemistry of pectins in shoot apical meristems: Consequences for intercellular adhesion. Protoplasma *225*, 15–22.
20. Louvet, R., Cavel, E., Gutierrez, L., Guenin, S., Roger, D., Gillet, F., Guerineau, F., and Pelloux, J. (2006). Comprehensive expression profiling of the pectin methylesterase gene family during silique development in Arabidopsis thaliana. Planta *224*, 782–791.
21. Galweiler, L., Guan, C., Muller, A., Wisman, E., Mendgen, K., Yephremov, A., and Palme, K. (1998). Regulation of polar auxin transport by AtPIN1 in Arabidopsis vascular tissue. Science *282*, 2226–2230.
22. Jiang, L., Yang, S.-L., Xie, L.-F., San Puah, C., Zhang, X.-Q., Yang, W.-C., Sundaresan, V., and Ye, D. (2005). Vanguard1 encodes a pectin methylesterase that enhances pollen tube growth in the Arabidopsis style and transmitting Tract. Plant Cell *17*, 584–596.
23. Röckel, N., Wolf, S., Kost, B., Rausch, T., and Greiner, S. (2008). Elaborate spatial patterning of cell-wall PME and PMEI at the pollen tube tip involves PMEI endocytosis, and reflects the distribution of esterified and de-esterified pectins. Plant J. *53*, 133–143.

24. Derbyshire, P., Findlay, K., McCann, M.C., and Roberts, K. (2007). Cell elongation in Arabidopsis hypocotyls involves dynamic changes in cell wall thickness. J. Exp. Bot. *58*, 2079–2089.
25. Cosgrove, D.J. (1999). Enzymes and other agents that enhance cell wall extensibility. Annu. Rev. Plant Physiol. Plant Mol. Biol. *50*, 391–417.
26. Spiro, M.D., Bowers, J.F., and Cosgrove, D.J. (2002). A comparison of oligogalacturonide- and auxin-induced extracellular alkalinization and growth responses in roots of intact cucumber seedlings. Plant Physiol. *130*, 895–903.
27. Deveaux, Y., Peaucelle, A., Roberts, G.R., Coen, E., Simon, R., Mizukami, Y., Traas, J., Murray, J.A., Doonan, J.H., and Laufs, P. (2003). The ethanol switch: A tool for tissue-specific gene induction during plant development. Plant J. *36*, 918–930.
28. Laufs, P., Peaucelle, A., Morin, H., and Traas, J. (2004). MicroRNA regulation of the CUC genes is required for boundary size control in Arabidopsis meristems. Development *131*, 4311–4322.
29. Peaucelle, A., Morin, H., Traas, J., and Laufs, P. (2007). Plants expressing a miR164-resistant CUC2 gene reveal the importance of post-meristematic maintenance of phyllotaxy in Arabidopsis. Development *134*, 1045–1050.
30. Liners, F., Letesson, J.J., Didembourg, C., and Van Cutsem, P. (1989). Monoclonal antibodies against pectin: Recognition of a conformation induced by calcium. Plant Physiol. *91*, 1419–1424.